



OPEN

Novel probe based on rhodamine B and quinoline as a naked-eye colorimetric probe for dual detection of nickel and hypochlorite ions

Seyyed Emad Hooshmand¹, Behnaz Baeiszadeh¹, Masoumeh Mohammadnejad²✉, Razieh Ghasemi³, Farshad Darvishi⁴, Ali Khatibi⁵, Morteza Shiri¹✉ & Faiq H. S. Hussain⁶✉

This work demonstrates the design and straightforward syntheses of several novel probe-based on rhodamine B and 2-mercaptoquinoline-3-carbaldehydes as a naked-eye colorimetric probe, indicating a sensitive and selective recognition towards nickel (II) with a limit of detection $0.30 \mu\text{mol L}^{-1}$ (0.02 mg L^{-1}). Further, by employing the oxidation property of hypochlorite (OCl^-), this novel probe parallelly has been deployed to detect hypochlorite in laboratory conditions with a limit of detection of $0.19 \mu\text{mol mL}^{-1}$ and in living cells. Regarded to negligible cell toxicity toward mammalian cells, this probe has the potential to determine these analytes in in-vivo investigation and foodstuff samples.

In the contemporary world, the issue of “prevention is better than cure” remains a highly contentious issue in therapeutic areas. One of the pivotal aspects of achieving this goal is the rapid detection of hazardous analysts in foods, water, and living organisms. With the sustainable improvement of the cosmopolitan metropolis, the severe problem of heavy metal pollution in the air, soil, and particularly in the water environment is cause for concern^{1–3}. Since the increase in water pollution could be considered an acute problem, rapid detection of heavy metal ion concentrations in drinking water is an effective remedy. One of these heavy metals that must be precisely taken into account is nickel. The transition series element nickel (Ni), which makes up around 3% of the earth’s composition, is the 24th most common element on the earth. At a non-dangerous level, nickel has advantages for instance an activator of some enzyme reactions and participating in critical metabolic systems³. However, the ingestion of nickel beyond acceptable levels induces the inhibition of oxidative enzyme activity, adverse effects on the lungs and kidneys, skin dermatitis, gastrointestinal distress, shortness of breath, and chest pain. It is really carcinogenic, and high levels of nickel cause the reduction of nitrogen and impaired growth. Based on World Health Organization (WHO), the maximum allowable level of nickel in potable water is 0.02 mg L^{-1} . Hence, it is tremendously important to augment a swift and straightforward method to implement selective and sensitive recognition of nickel ions. Besides that, hypochlorite fulfills a key role in defending against the invasion of pathogens. Nevertheless, an excessive amount of hypochlorite preparation induces several diseases, namely kidney disease, arthritis, osteoarthritis, atherosclerosis, and cancer^{5,6}. Consequently, rapid recognition HOCl/OCl^- in vitro and in vivo is really imperative. Moreover, since hypochlorite is commonly deployed as a disinfection of drinking water and household bleach, a high concentration of hypochlorite must be damaging humans and animals, causing nose irritation or arousing eye and stomach discomfort. Owing to the destructive influence of hypochlorite, it is essential to swiftly detect and monitor OCl^- residues^{7–9}.

The sensor as well as probe fields as privileged tools for clinical diagnostics has paved the way for developing earlier diagnoses and treatments. Most popular approaches for detecting nickel rely on electrochemical methods,

¹Department of Organic Chemistry, Faculty of Chemistry, Alzahra University, Vanak, Tehran 1993893973, Iran. ²Department of Analytical Chemistry, Faculty of Chemistry, Alzahra University, Vanak, Tehran 1993893973, Iran. ³Department of Nanotechnology, Jabir Ibn Hayyan Institute, Technical and Vocational Training Organization, Isfahan, Iran. ⁴Department of Microbiology, Faculty of Biological Sciences, Alzahra University, Tehran, Iran. ⁵Department of Biotechnology, Faculty of Biological Sciences, Alzahra University, Tehran, Iran. ⁶Department of Medical Analysis, Faculty of Applied Science, Tishk International University-Erbil, Kurdistan Region, Iraq. ✉email: m.mohammadnejad@alzahra.ac.ir; mshiri@alzahra.ac.ir; faiq.hussain@tiu.edu.iq

atomic absorption spectroscopy, and inductive coupled plasma atomic emission spectrometry (ICP-AES) for declining the interference impacts^{10–12}. In spite of the great capability of the atomic techniques in selective detections, these methods have drawbacks such as their wrecking strategies, high cost as well as long-time analysis. The rational design of the naked-eye colorimetric probe as a swift and visual way culminates in detecting detrimental heavy metals and any imperative analytes^{13,14}. Although many colourimetric sensors have been introduced for heavy metals such as mercury and cadmium or copper, there are very few published reports about nickel. In this line, Jiang et al.¹⁵ devised a novel coumarin-based colourimetric nickel sensor with high sensitivity and selectivity toward Ni²⁺ ion. Yang's research group reported Two novel pyrazole-based chemosensors that illustrate high sensitivity and selectivity for detecting nickel¹⁶. Moreover, Zhang and coworkers demonstrated a colorimetric and naked-eye chemosensor based on quinoline and 2-naphthol with detect Ni²⁺ in aqueous solution with specific selectivity and high sensitivity¹⁷. In this area, rhodamine B reveals a wealth of opportunities for chemosensor and probe applications, and several small molecules and macromolecules-centered rhodamine B have recently been introduced as an elevated probe for mercury¹⁸, zinc¹⁹, copper²⁰, lead²¹, iron²², picric acid²³, and fluoride²⁴. Rhodamine-centered probe universally are non-fluorescent and relatively colorless, notwithstanding they exhibit a color change to deep pink. When they are placed in an acidic solution, they demonstrate a strong fluorescence²⁵. This observation is owing to protonation at the carbonyl group, and following ring-opening of its spirolactam scaffold²⁶. Metals ions could cause changing the color and fluorescence by assuming a role resembling that of the hydrogen ions in acidic solvents, providing that a suitable ligand is exhibited on the spirolactam ring²⁷. As a result, in the present study, in continuation of our study on quinoline chemistry^{28–38}, we made an effort to enhance a novel probe based on rhodamine B and quinoline as a naked-eye colorimetric probe that could be efficiently and selectively deployed for detecting heavy metals, namely nickel and also hypochlorite. In addition to that, the chemodosimeter of the novel rhodamine-based probe for analyte with high sensitivity showed a drastic color change from colorless to deep pink after the addition of the analyte³⁹. To the best of our knowledge, this is the first time that a dual colourimetric probe for nickel and hypochlorite ions is devised.

Experimental

Reagents and instruments

The chemicals such as Nickel chloride, rhodamine B, and hydrazine were prepared by Aldrich. The solvents were analytical grade and purchased from Merck. Deionized water was used for the dilution of the solutions. The absorbance measurement was carried out by double-beam UV-Vis spectrophotometer using a 1 cm quartz cell (Perkin-Elmer, Lambda 35, USA). The fluorescence measurement was carried out by a PI spectrophotometer using a 1 cm quartz cell (Cary Eclipse Agilent G980A). ¹H-NMR and ¹³C-NMR spectra were recorded on Bruker AQS AVANCE 500, 400, and 300 MHz spectrometers respectively, using TMS as an internal standard and DMSO-d₆ and CDCl₃ as solvent.

General synthesis of probe based on rhodamine B and quinoline

In a 50 ml flask, 1 mmol (0.203 g) of the 2-mercapto-6-methyl quinoline-3-carbaldehyde compound and 1 mmol (0.465 g) rhodamine B hydrazide under reflux conditions and nitrogen atmosphere in methanol were mixed by a magnetic stirrer. The progress of the reaction was monitored by TLC in the mixture of n-hexane and ethyl acetate in a ratio of 6:4, the reaction was completed after 24 h. The resulting precipitates were purified by washing with methanol and the final product **7a** was obtained as a yellow precipitate with a yield of 85%.

Results and discussion

After facile synthesis of rhodamine hydrazide²⁰ and 2-mercaptoquinoline-3-carbaldehydes⁴⁰ based on previous reports, we commenced our work by the addition of rhodamine hydrazide with 2-mercaptoquinoline-3-carbaldehydes in MeOH under refluxing conditions yields the novel rhodamine-based probe with appropriate yield (Fig. 1). Next, the synthetic rhodamine-based probe was characterized by FTIR, ¹H-NMR, and ¹³C-NMR.

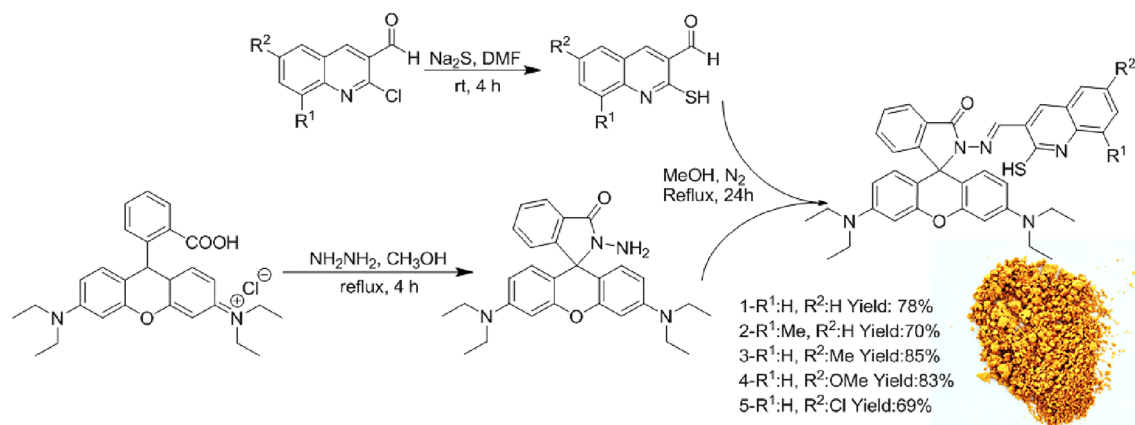


Figure 1. Synthesis of novel rhodamine-based probe.

The interaction between a synthesized rhodamine-based probe and several metal ions (Fig. 2a) was investigated using the same settings. It was clear that the addition of an extensive diversity of environmentally metal ions namely Cu^{2+} , Pb^{2+} , Zr^{2+} , Zn^{2+} , Ag^+ , Al^{3+} , Hg^{2+} , Co^{2+} , Mn^{2+} , Cr^{3+} , Sn^{2+} , Fe^{3+} , Cd^{2+} , Al^{3+} , Pd^{3+} , Fe^{2+} , Ca^{2+} , Ba^{2+} , Mn^{2+} , Ni^{2+} , did not have as a quite much effect on the probe as Ni^{2+} (Fig. 2b). The outcome supported the high selectivity of the novel probe which is considered a pivotal characteristic of an ion-selective probe. Figure 2c depicts the UV–visible absorption spectra of this new probe in the absence and presence of Ni^{2+} . Ni^{2+} could chelate with the probe, causing a ring-opening reaction of its spirolactam scaffold, and then coordinate with carbonyl oxygen, nitrogen atoms of two imine groups, and quinoline nitrogen when added to the probe solution²⁵. It resulted in a blue shift in the absorption spectrum, the formation of a new band at 560 nm, and a steady rise in absorbance with increasing Ni^{2+} concentration. Consequently, the probe solution changed from yellow to deep pink.

For investigation of the interaction of Ni^{2+} with novel rhodamine and quinoline-based probe, various concentrations of this element solution were added to the solution and absorbance spectra were recorded up to 30 min. By increasing the concentration of Ni, the new peak at 560 nm was observed, and the intensity increased steadily. The absorption spectra are illustrated in Fig. 3a. As a matter of fact, the intensity of the absorbance at 560 nm pertaining to the addition of Ni^{2+} concentration drastically, and the calibration curve was plotted based on the absorbance increasing at 560 nm in the presence of Ni^{2+} (Fig. 3b) in the range of $0.1\text{--}0.8 \times 10^{-5} \text{ mol L}^{-1}$ with a detection limit of $0.03 \times 10^{-5} \text{ mol L}^{-1}$. The color of the solution swiftly changed from yellow to deep pink which can be rapidly diagnosed by the naked eye. A color gradient from yellow to deep pink was obviously perceived upon increasing the concentration of nickel which permitted a semiquantitative detection of the analyte in water

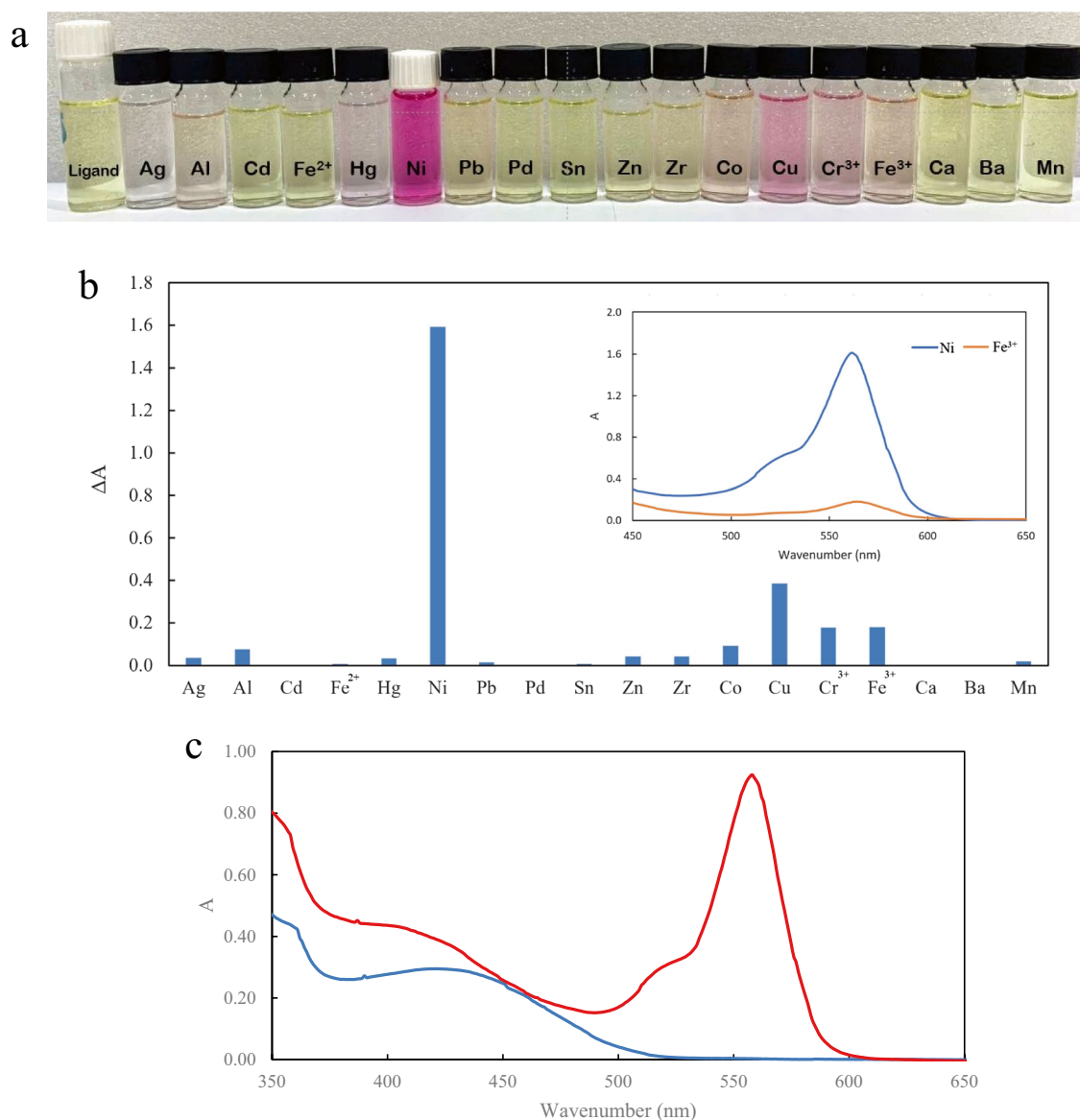


Figure 2. (a) Photographic images of colorimetric detection of various metals in water through simple naked-eye analysis. (b) Absorbance changes of the novel rhodamine-based probe in the presence of various metal ions and for example UV–visible spectra in the presence of Ni^{2+} and Fe^{3+} (inserted). (c) The UV–visible absorption spectra of the probe in the absence (blue) and presence (red) of Ni^{2+} .

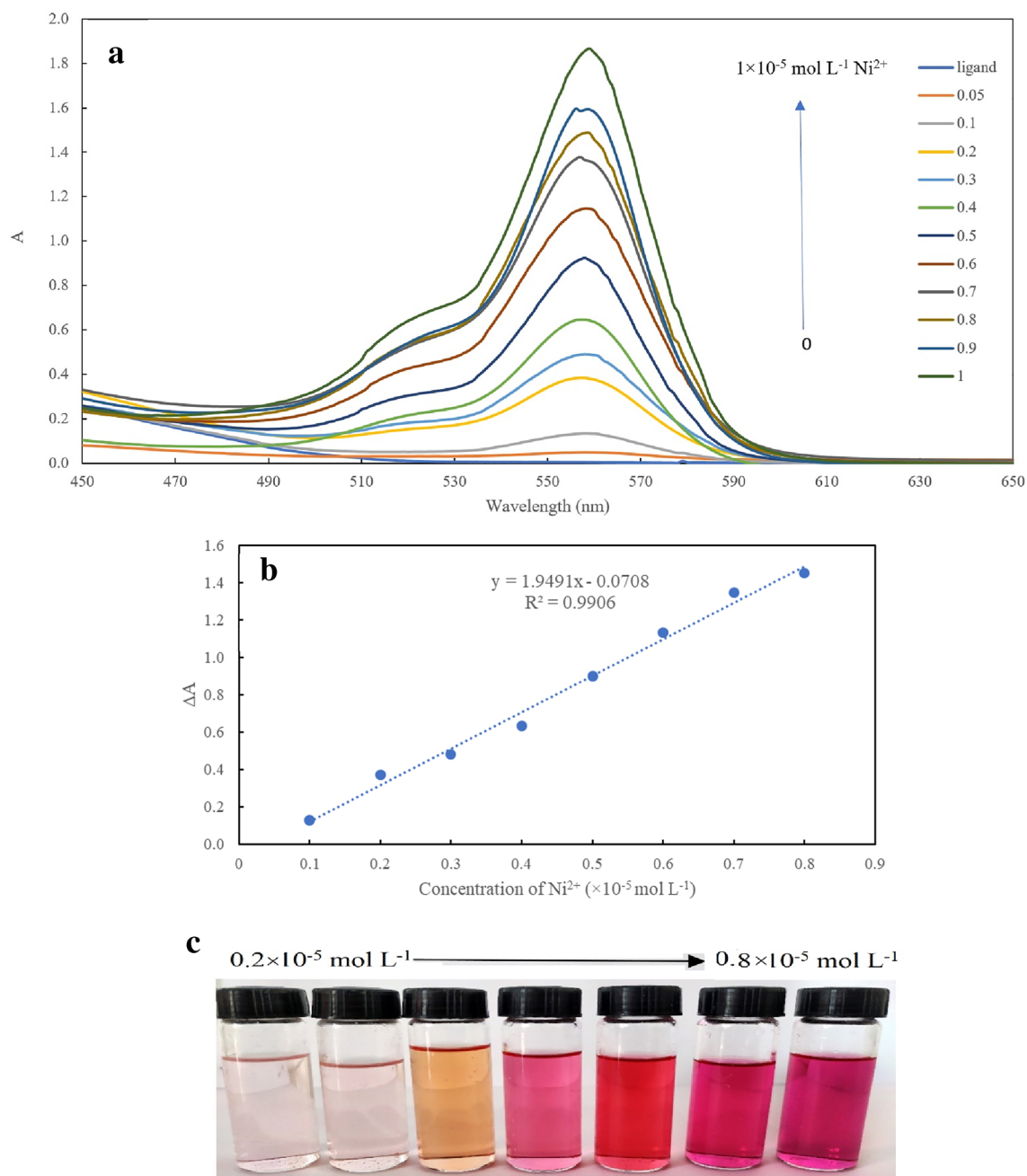


Figure 3. (a) Absorption spectra of rhodamine-based probe (5×10^{-5} M) with the addition of Ni ($0.05, 0.1, 0.2, 0.3, 0.4, 0.5, 0.6, 0.7, 0.8, 0.9, 1 \times 10^{-5}$ M); (b) linearity of absorbance intensity of rhodamine-based probe with Ni from 0.1 to 0.8×10^{-5} M. (c) Photographic images of colorimetric detection of nickel (0.2 – 0.8×10^{-5} mol L⁻¹) in water through simple naked-eye analysis.

by swift and facile visual analysis (Fig. 3c). Evidently, the color intensity became stronger with increasing the concentration of Ni²⁺.

To study the selectivity of the synthesized probe, the effect of different cations and anions such as Cu²⁺, Pb²⁺, Zr²⁺, Zn²⁺, Ag⁺, Al³⁺, Hg²⁺, Co²⁺, Mn²⁺, Cr³⁺, Sn²⁺, Fe³⁺, Cd²⁺, Al³⁺, Pd³⁺, Fe²⁺, Ca²⁺, Ba²⁺, Mn²⁺, Cl⁻, NO₃⁻, PO₄³⁻, S²⁻ and SO₄²⁻ on determination of Ni²⁺ was investigated. Different concentration of these ions were added to the probe-Ni solutions and the absorption spectra of rhodamine-based probe were recorded. The tolerance limit of an ion was taken as the maximum amount of the ion causing an error not greater than ± 5%. A 100-fold excess of these cation and anions did not interfere on the determination of Ni²⁺ and the major interference was Cu²⁺ (Fig. 4). The interfering effect of Cu²⁺, was successfully removed by addition of dilute sulfide solution into the sample solution.

Moreover, the role of functional groups in this naked-eye colorimetric probe was perused. Accordingly, in addition to 2-mercaptoquinoline-3-carbaldehydes, 2-chloroquinoline-3-carbaldehyde and

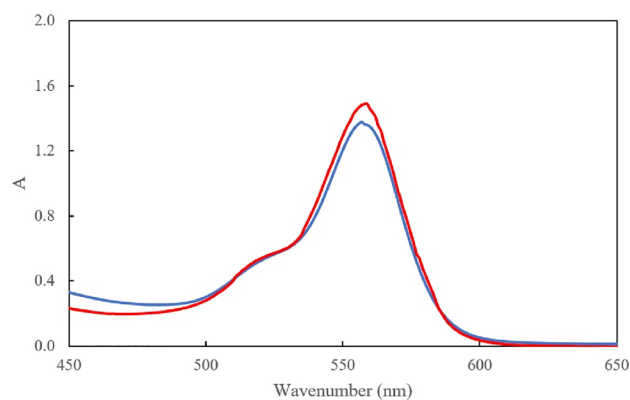


Figure 4. Absorption spectra of rhodamine-based probe with Ni^{2+} (blue spectrum) and the spectra of this solution (probe and Ni^{2+}) in the presence of Cu^{2+} .

2-hydroxyquinoline-3-carbaldehyde have been deployed in this project. As expected, on account of the appropriate affinity of mercaptans with such metals, a rhodamine-based probe prepared by 2-mercaptoquinoline-3-carbaldehydes revealed elevated interaction with nickel in comparison with hydroxy and chloro derivatives. (Fig. 5) Furthermore, different 2-mercaptoquinoline-3-carbaldehydes were used in probe scaffolds and subsequently the interaction of probe-encompassing substitutions namely methyl, methoxy or chlorine with Ni^{2+} were investigated. The outcome depicted the elevated tendency of the probe prepared by 2-mercapto-6-methylquinoline-3-carbaldehyde to the analyte than the other derivatives (Fig. 6).

In addition, based on the structure of the synthesized component, its fluorescence spectra were recorded in the presence of different ions with $\lambda_{\text{ex}} = 310 \text{ nm}$ (Fig. 7 inset). The fluorescence spectrum of the synthesized component shows a very low fluorescence intensity in $\lambda_{\text{em}} = 590 \text{ nm}$ that is dramatically increase in the presence of Ni^{2+} compared to some other metal ions. These fluorescence results confirm the absorbance changes of probe by Ni^{2+} .

Detection of hypochlorite

To study the interaction of the probe by ClO^- , the fluorescence properties of the synthesized component were recorded. The fluorescent titration profiles of the probe ($5 \times 10^{-5} \text{ M}$) with ClO^- ($0.05\text{--}1 \times 10^{-5} \text{ M}$) are illustrated in Fig. 8a. As the concentration of ClO^- was titrated into the probe, there was a noticeable fluorescence amplification at $\lambda_{\text{em}} = 410$ and 590 nm (with $\lambda_{\text{ex}} = 310 \text{ nm}$). The ring-opening rhodamine acid caused by the interaction of the probe rhodamine B-based probe with ClO^- is another possible explanation for the outcomes. Additionally, the probe rhodamine B-based probe exhibits remarkable linearity between fluorescence intensity (at $\lambda_{\text{em}} = 410 \text{ nm}$) and ClO^- concentration across the range of $0.05\text{--}0.9 \times 10^{-5} \text{ M}$ (Fig. 8b). The detection limit was calculated at $0.19 \mu\text{M}$, which also demonstrated a highly sensitive characteristic. This outcome suggests that the probe may be used to quantitatively detect HOCl/ClO^- .

The observed changes in the absorption and emission colours of the probe upon the addition of OCl^- can be attributed to the opening of the spirolactam ring in the rhodamine motif. In most cases, the process of ring opening in cations is facilitated by the chelation of cations with the rhodamine-linked derivative. This leads to the creation of a chelation-enhanced colorimetric and fluorescence probe, which can detect various metal ions. The

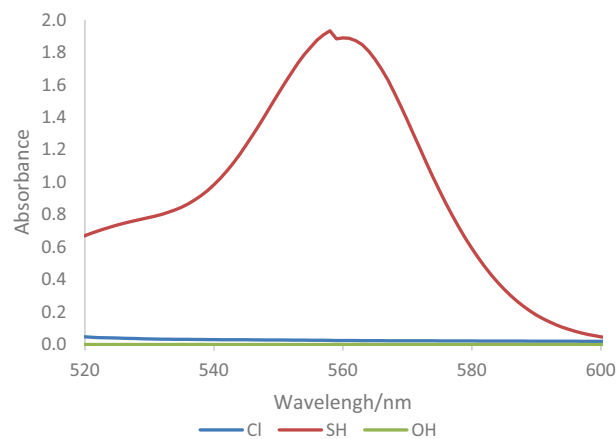


Figure 5. Effect of substitutions of position 2 of quinoline-3-carbaldehydes in performance of novel rhodamine-based probes.

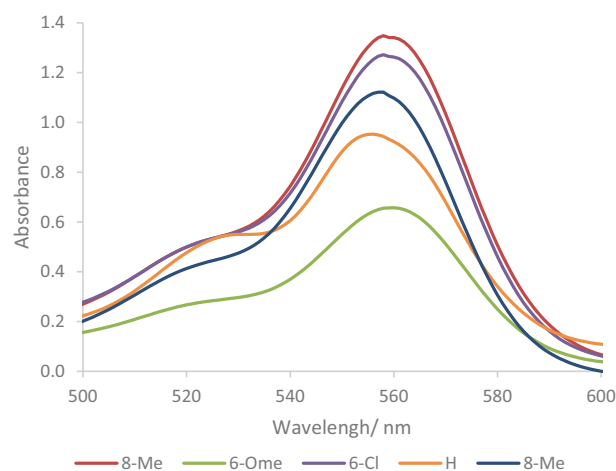


Figure 6. Effect of substitutions on 2-mercaptoquinoline-3-carbaldehydes in performance of novel rhodamine-based probes.

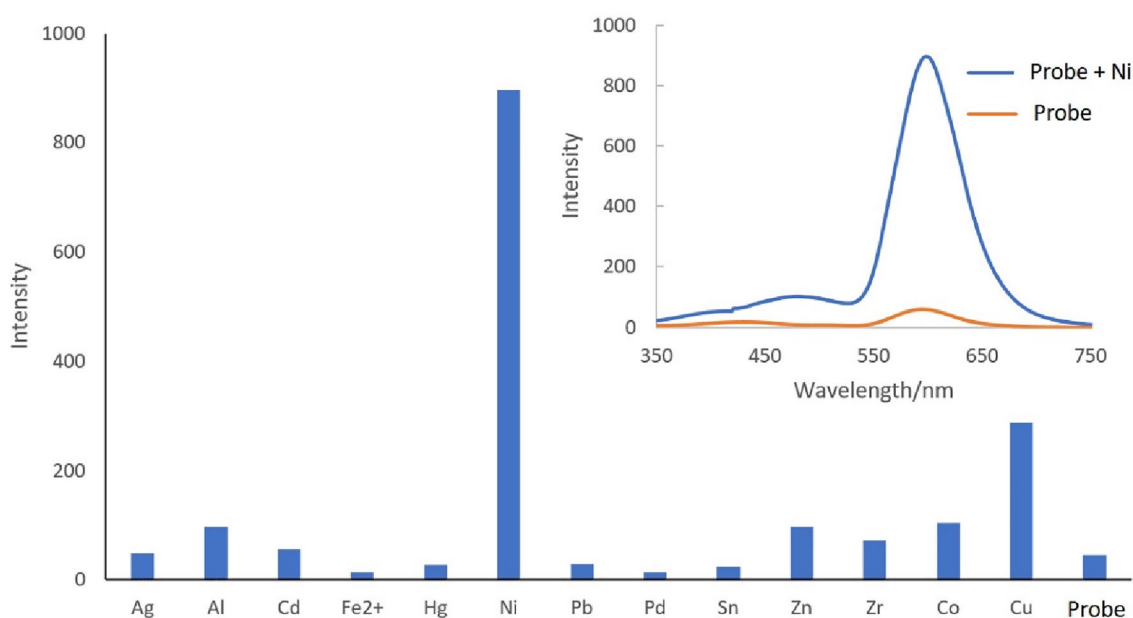


Figure 7. Fluorescence intensity of probe in the presence of different metal ions (inset: fluorescence spectra of probe and probe-Ni).

probe operates by converting the spirolactam form of the rhodamine dye (which is colorless and nonfluorescent) to the ring-open amide form (which is deep pink colored and exhibits strong fluorescence)^{41–44}.

To study the effect of different anions on the ClO^- determination, different anions such as Cl^- , NO_3^- , PO_4^{3-} , SO_4^{2-} and S^{2-} was studied in selectivity of the synthesized probe. Based on the results, these anions do not show effect on the signal up to 1000 order of ClO^- concentration.

The novel probe function in living cells

The yeast cells of *Saccharomyces cerevisiae* ATCC9763 were treated with two different concentrations (10^{-4} and 10^{-5} M) of the probe. The probe was not observed inside yeast cells by fluorescence microscopy. To determine the function of the novel probe in mammalian cells and its cell viability and cytotoxicity, the breast cancer MCF7 cells were treated with two concentrations (10^{-4} and 10^{-5} M) of the probe. Images of fluorescence microscopy show that the probe has entered the cells. Therefore, a probe rhodamine B-based probe can be used for fluorescence microscopy imaging of MCF7 cells (Fig. 9a).

As shown in Fig. 9b, the cell viability and cell toxicity were obtained at 97.59% and 2.4%, and 75.16% and 24.83% for 10^{-5} and 10^{-4} M concentration respectively after 24 h via MTT assay. The results show that the cell viability decreases when the concentration of the probe increases, but this change is not very significant, and the probe has no cytotoxicity for MCF7 cells.

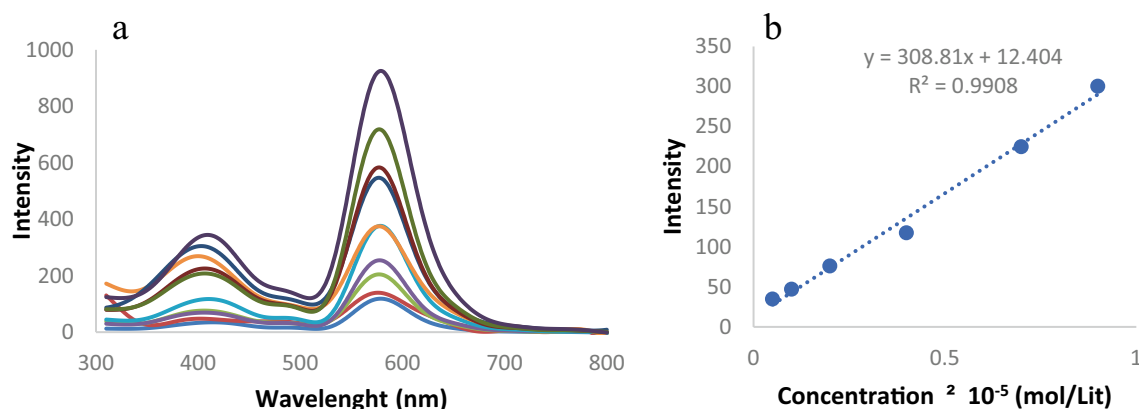


Figure 8. (a) Fluorescence spectra of probe rhodamine B-based probe (5×10^{-5} M) with the addition of ClO^- ($0.05, 0.1, 0.2, 0.3, 0.4, 0.5, 0.6, 0.7, 0.8, 0.9, 1 \times 10^{-5}$ M). (b) Linearity of fluorescence intensity of rhodamine B-based probe with ClO^- .

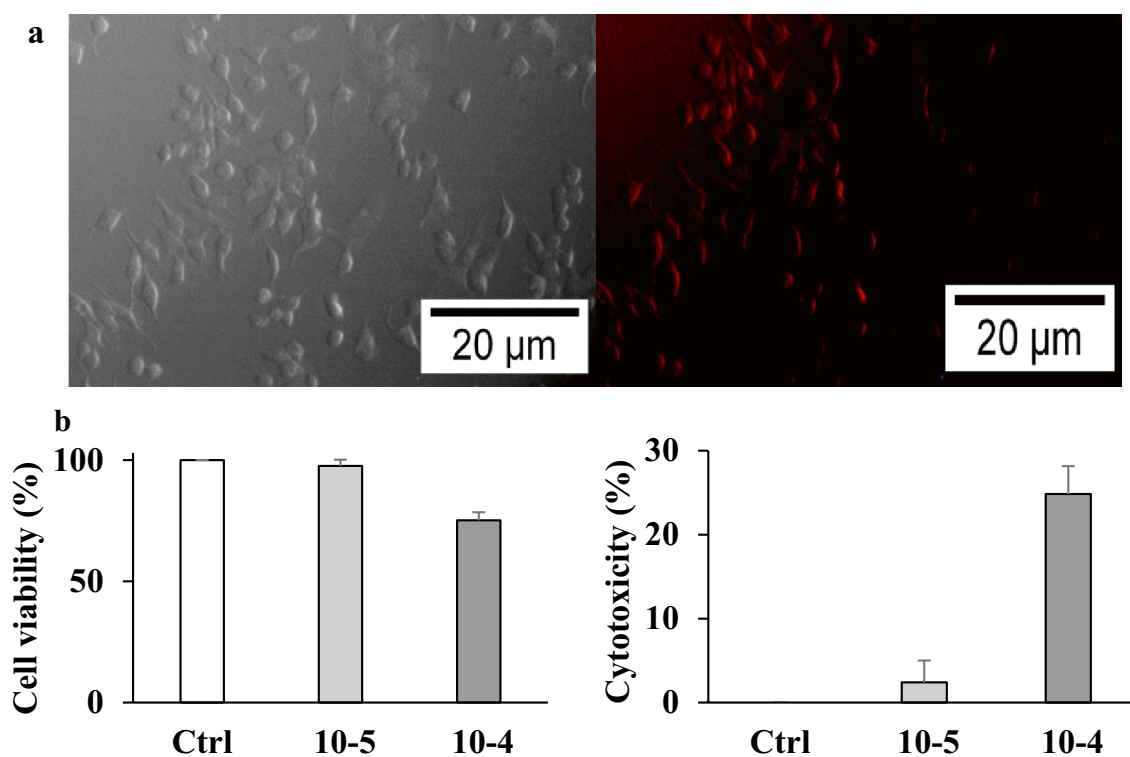


Figure 9. (a) Light and fluorescence images of MCF7 cells treated with the rhodamine B-based probe. (b) Cell viability and cytotoxicity effects of two concentrations (10^{-4} and 10^{-5} M) of the probe on MCF7 cells after 24 h.

Conclusion

Here, we have devised a highly efficient novel probe based on rhodamine B and 2-mercaptoquinoline-3-carbaldehydes for dual sensing heavy metals and hypochlorite. The probe depicted a significant color change from colorless to pink and fluorescence improvement upon the addition of nickel and ClO^- ions. The probe moreover had a low limit of detection ($0.3 \mu\text{mol mL}^{-1}$ for nickel and $0.19 \mu\text{mol mL}^{-1}$ for ClO^- ions). Considering negligible toxicity toward mammalian cells and the successful application of this novel probe as an imaging agent for endogenous hypochlorite in living cells, this probe-centered rhodamine could promisingly be used in industrial applications and foodstuff samples.

Data availability

All data generated or analyzed during this study are included in this published article [and its Supplementary Information file].

References

- Mohammed, A. S., Kapri, A. & Goel, R. *Bio-management of Metal-Contaminated Soils 1–28* (Springer, 2011).
- Briffa, J., Sinagra, E. & Blundell, R. Heavy metal pollution in the environment and their toxicological effects on humans. *Heliyon* **6**, e04691 (2020).
- Raval, N. P., Shah, P. U. & Shah, N. K. Adsorptive removal of nickel (II) ions from aqueous environment: A review. *J. Environ. Manag.* **179**, 1–20 (2016).
- Acheampong, M. A., Pereira, J. P., Meulepas, R. J. & Lens, P. N. Kinetics modelling of Cu (II) biosorption on to coconut shell and *Moringa oleifera* seeds from tropical regions. *Environ. Technol.* **33**, 409–417 (2012).
- Tang, Z., Ding, X.-L., Liu, Y., Zhao, Z.-M. & Zhao, B.-X. A new probe based on rhodamine B and benzothiazole hydrazine for sensing hypochlorite in living cells and real water samples. *RSC Adv.* **5**, 99664–99668 (2015).
- Prokopowicz, Z. M. *et al.* Hypochlorous acid: A natural adjuvant that facilitates antigen processing, cross-priming, and the induction of adaptive immunity. *J. Immunol.* **184**, 824–835 (2010).
- Shi, W.-J. *et al.* A BODIPY-based “OFF-ON” fluorescent probe for fast and selective detection of hypochlorite in living cells. *Dyes Pigm.* **170**, 107566 (2019).
- Li, H. *et al.* A mitochondria-targeted fluorescent probe for fast detecting hypochlorite in living cells. *Dyes Pigm.* **176**, 108192 (2020).
- Wang, X., Song, F. & Peng, X. A versatile fluorescent probe for imaging viscosity and hypochlorite in living cells. *Dyes Pigm.* **125**, 89–94 (2016).
- Şahin, Ç. A., Efeçinar, M. & Şatıroğlu, N. Combination of cloud point extraction and flame atomic absorption spectrometry for preconcentration and determination of nickel and manganese ions in water and food samples. *J. Hazard. Mater.* **176**, 672–677 (2010).
- Dos Anjos, S. L. *et al.* Multivariate optimization of a procedure employing microwave-assisted digestion for the determination of nickel and vanadium in crude oil by ICP OES. *Talanta* **178**, 842–846 (2018).
- Mirabi, A., Rad, A. S. & Nourani, S. Application of modified magnetic nanoparticles as a sorbent for preconcentration and determination of nickel ions in food and environmental water samples. *TRAC Trends Anal. Chem.* **74**, 146–151 (2015).
- Khattab, T. A. *et al.* Fabrication of PAN-TCF-hydrazone nanofibers by solution blowing spinning technique: Naked-eye colorimetric sensor. *J. Environ. Chem. Eng.* **5**, 2515–2523 (2017).
- Aghayan, M., Mahmoudi, A., Sazegar, M. R. & Adhami, F. A novel colorimetric sensor for naked-eye detection of cysteine and Hg²⁺ based on “on-off” strategy using Co/Zn-grafted mesoporous silica nanoparticles. *Dalton Trans.* **50**, 13345–13356 (2021).
- Jiang, J., Gou, C., Luo, J., Yi, C. & Liu, X. A novel highly selective colorimetric sensor for Ni (II) ion using coumarin derivatives. *Inorganic Chem. Commun.* **15**, 12–15 (2012).
- Yang, G. *et al.* Two novel pyrazole-based chemosensors: “naked-eye” colorimetric recognition of Ni²⁺ and Al³⁺ in alcohol and aqueous DMF media. *New J. Chem.* **42**, 14630–14641 (2018).
- Liu, X., Lin, Q., Wei, T.-B. & Zhang, Y.-M. A highly selective colorimetric chemosensor for detection of nickel ions in aqueous solution. *New J. Chem.* **38**, 1418–1423 (2014).
- Hong, M., Chen, Y., Zhang, Y. & Xu, D. A novel rhodamine-based Hg²⁺ sensor with a simple structure and fine performance. *Analyst* **144**, 7351–7358 (2019).
- Wechakorn, K., Suksen, K., Piyachaturawat, P. & Kongsaree, P. Rhodamine-based fluorescent and colorimetric sensor for zinc and its application in bioimaging. *Sens. Actuators B: Chem.* **228**, 270–277 (2016).
- Mohammadnejad, M., Shiri, M., Heydari, M., Faghihi, Z. & Afshinpoor, L. A novel high selective colorimetric chemosensor for determination of copper in food samples: Visual detection. *Chem. Select* **5**, 13690–13693 (2020).
- Sunnapu, O., Kotla, N. G., Maddiboyina, B., Singaravadi, S. & Sivaraman, G. A rhodamine based “turn-on” fluorescent probe for Pb (II) and live cell imaging. *RSC Adv.* **6**, 656–660 (2015).
- Cheredy, N. R., Suman, K., Korrapati, P. S., Thennarasu, S. & Mandal, A. B. Design and synthesis of rhodamine based chemosensors for the detection of Fe³⁺ ions. *Dyes Pigments* **95**, 606–613 (2012).
- Sivaraman, G., Vidya, B. & Chellappa, D. Rhodamine based selective turn-on sensing of picric acid. *RSC Adv.* **4**, 30828–30831 (2014).
- Sivaraman, G. & Chellappa, D. Rhodamine based sensor for naked-eye detection and live cell imaging of fluoride ions. *J. Mater. Chem. B* **1**, 5768–5772 (2013).
- Kim, H. N., Lee, M. H., Kim, H. J., Kim, J. S. & Yoon, J. A new trend in rhodamine-based chemosensors: Application of spirolactam ring-opening to sensing ions. *Chem. Soc. Rev.* **37**, 1465–1472 (2008).
- Sivaraman, G., Anand, T. & Chellappa, D. Turn-on fluorescent chemosensor for Zn (II) via ring opening of rhodamine spirolactam and their live cell imaging. *Analyst* **137**, 5881–5884 (2012).
- Milindanuth, P. & Pisitsak, P. A novel colorimetric sensor based on rhodamine-B derivative and bacterial cellulose for the detection of Cu (II) ions in water. *Mater. Chem. Phys.* **216**, 325–331 (2018).
- Shiri, M., Fathollahi-Lahroud, M. & Yasaei, Z. A novel strategy for the synthesis of 6H-chromeno [4,3-b] quinoline by intramolecular Heck cyclization. *Tetrahedron* **73**, 2501–2503 (2017).
- Shiri, M., Ranjbar, M., Yasaei, Z., Zamanian, F. & Notash, B. Palladium-catalyzed tandem reaction of 2-chloroquinoline-3-carbaldehydes and isocyanides. *Org. Biomol. Chem.* **15**, 10073 (2017).
- Salehi, P. & Shiri, M. Palladium-catalyzed regioselective synthesis of 3-(hetero)arylpropynamides from gem-dibromoalkenes and isocyanides. *Adv. Synth. Catal.* **361**, 118–125 (2019).
- Shiri, M. *et al.* Highly selective synthesis of α -hydroxy, -oxy, and -oxoamides via post-Passerini condensation transformation. *Synthesis* **52**, 3243–3252 (2020).
- Shiri, M., Gholami-Koupaei, Z., Kaffash, S. & Yasaei, Z. Palladium catalyzed domino Sonogashira coupling of 2-chloro-3-(chloromethyl)quinolines with terminal acetylenes followed by dimerization. *Polycycl. Aromat. Comp.* **41**, 1722–1728 (2021).
- Shiri, M., Salehi, P., Mohammadpour, Z., Salehi, P. & Notash, B. Cs₂CO₃-mediated regio- and stereoselective sulfonylation of 1,1-dibromo-1-alkenes and sodium sulfonates. *Synthesis* **52**, 1149–1156 (2021).
- Salehi, P., Tanbakouchian, Z., Farajinia-Lehi, N. & Shiri, M. Cascade synthesis of 2,4-disulfonylpyrroles by the sulfonylation/[2+3]-cycloaddition reactions of gem-dibromoalkenes with arylsulfonyl methyl isocyanides. *RSC Adv.* **11**, 13292–13296 (2021).
- Tonekaboni, M. S., Tanbakouchian, Z., Majedi, S. & Shiri, M. Synthesis of [1,4]oxathiepin[5,6-b]quinolines via base-mediated intramolecular hydroalkoxylation. *SynOpen* **199**, 110–106 (2022).
- Bandehali-Naeini, F., Shiri, M., Ramezani, B. & Rajai-Daryasarei, S. Quinoline-based polyazaheterocycles by a hydrogen peroxide-mediated isocyanide insertion. *Polycycl. Aromat. Comp.* **41**, 676–684 (2021).
- Tanbakouchian, Z., Zolfigol, M. A., Notash, B., Ranjbar, M. & Shiri, M. Synthesis of four series of quinoline-based heterocycles by reacting 2-chloroquinoline-3-carbonitriles with various types of isocyanides. *Appl. Organomet. Chem.* **2019**, e5024 (2019).
- Yasaei, Z., Mohammadpour, Z., Shiri, M., Tanbakouchian, Z. & Fazelzadeh, S. Isocyanide reactions toward the synthesis of 3-(oxazol-5-yl)quinoline-2-carboxamides and 5-(2-tosylquinolin-3-yl)oxazole. *Front. Chem.* **7**, 433 (2019).

39. Parmar, N. J., Barad, H. A., Labana, B. M., Kant, R. & Gupta, V. K. A glycerol mediated domino reaction: An efficient, green synthesis of polyheterocycles incorporating a new thiochromeno [2, 3-b] quinoline unit. *RSC Adv.* **3**, 20719–20725 (2013).
40. Shiri, M. *et al.* The synthesis of iminothiophenone-fused quinolines and evaluation of their serendipitous reactions. *RSC Adv.* **6**, 92235 (2016).
41. Yuan, L., Lin, W., Chen, B. & Xie, Y. Development of FRET-based ratiometric fluorescent Cu²⁺ chemodosimeters and the applications for living cell imaging. *Org. Lett.* **14**, 432 (2012).
42. Kumar, M., Kumar, N., Bhalla, V., Sharma, P. R. & Kaur, T. Highly selective fluorescence turn-on chemodosimeter based on rhodamine for nanomolar detection of copper ions. *Org. Lett.* **14**, 406 (2012).
43. Zhang, J. F. *et al.* Naphthalimide modified rhodamine derivative: Ratiometric and selective fluorescent sensor for Cu²⁺ based on two different approaches. *Org. Lett.* **12**, 3852 (2010).
44. Goswami, S. *et al.* Nanomolar detection of hypochlorite by a rhodamine-based chiral hydrazide in absolute aqueous media: Application in tap water analysis with live-cell imaging. *Anal. Chem.* **86**, 6315 (2014).

Acknowledgements

We are grateful for financial support provided by Alzahra University and the Iran National Science Foundation (INSF).

Author contributions

S.E.H.: conceptualization, formal analysis, methodology, writing—original draft; B.B.: data curation, investigation, software; M.M.: formal analysis, validation, visualization; R.G.: investigation, methodology; F.D. and A.K.: resources, validation, visualization; M.S.: conceptualization, project administration, resources, supervision, validation, writing—review & editing; F. S.H.: conceptualization, formal analysis, data curation, writing—review & editing.

Competing interests

The authors declare no competing interests.

Additional information

Supplementary Information The online version contains supplementary material available at <https://doi.org/10.1038/s41598-023-44395-x>.

Correspondence and requests for materials should be addressed to M.M., M.S. or F.H.S.H.

Reprints and permissions information is available at www.nature.com/reprints.

Publisher's note Springer Nature remains neutral with regard to jurisdictional claims in published maps and institutional affiliations.



Open Access This article is licensed under a Creative Commons Attribution 4.0 International License, which permits use, sharing, adaptation, distribution and reproduction in any medium or format, as long as you give appropriate credit to the original author(s) and the source, provide a link to the Creative Commons licence, and indicate if changes were made. The images or other third party material in this article are included in the article's Creative Commons licence, unless indicated otherwise in a credit line to the material. If material is not included in the article's Creative Commons licence and your intended use is not permitted by statutory regulation or exceeds the permitted use, you will need to obtain permission directly from the copyright holder. To view a copy of this licence, visit <http://creativecommons.org/licenses/by/4.0/>.

© The Author(s) 2023